

THE INFLUENCE OF COOLING RATE ON THE STRUCTURE AND MECHANICAL PROPERTIES OF $\text{Al}_4\text{CoCrCuFeNi}$ MULTICOMPONENT ALLOY

O. I. Kushnerov^{1*}, V. F. Bashev², S. I. Ryabtsev¹

¹*Oles Honchar Dnipro National University, Dnipro, Ukraine*

²*Dniprovsky State Technical University, Kamianske, Ukraine*

**e-mail: kushnrv@gmail.com*

The present study focused on examining the composition, structure, and mechanical properties of an $\text{Al}_4\text{CoCrCuFeNi}$ multicomponent high-entropy alloy. Two states of the alloy, namely as-cast and melt-quenched, were investigated. The composition of the alloy was determined based on established criteria found in literature, which consider factors such as entropy, enthalpy of mixing, valence electron concentration, and atomic size difference of the components. To synthesize the alloy films, a splat-quenching technique was employed, where the films were rapidly cooled from the molten state. The estimated cooling rate of the films was approximately 10^6 K/s, calculated based on the film thickness. X-ray diffraction analysis was conducted on both the as-cast and melt-quenched $\text{Al}_4\text{CoCrCuFeNi}$ alloy samples, revealing that they exhibited an ordered B2 phase in their structure. The microhardness measurements were carried out to evaluate the mechanical properties of the alloy. The as-cast alloy displayed a microhardness of 6500 MPa, while the melt-quenched film exhibited a significantly higher microhardness, reaching 9400 MPa.

Keywords: high-entropy alloy, microstructure, phase composition, melt-quenching, microhardness.

Received 03.11.2023; Received in revised form 30.12.2023; Accepted 15.12.2023

1. Introduction

High-entropy alloys (HEAs) are a new class of metal materials that have multiple principal elements in equal or near-equal proportions. They have attracted a lot of attention in materials science and engineering because of their unique properties and potential applications [1-4]. Unlike conventional alloys, which are based on one or two dominant elements with minor additions of other elements, HEAs have a high configurational entropy that favors the formation of simple solid solutions with face-centered cubic (FCC), body-centered cubic (BCC) or hexagonal close-packed (HCP) structures. Some authors have suggested that only equimolar alloys with simple solid solutions of BCC and FCC crystal lattices should be classified as HEAs. For other alloys with high entropy but with non-equimolar compositions or more complex phase structures, which may include ordered solid solutions and intermetallic compounds, new terms have been proposed, such as complex concentrated alloys (CCA) or multi-principal element alloys (MPEA) [4].

Among the advantages of high-entropy alloys are high strength, excellent high-temperature performance, good ductility, and fracture toughness at low temperatures, enhanced corrosion and oxidation resistance, shape memory effect [1-6]. HEAs can be designed by selecting elements from different groups of the periodic table. The number of possible compositions for HEAs is much larger than that for conventional alloys, which opens new possibilities for exploring novel materials with tailored properties.

HEAs can be synthesized by various methods, such as casting, powder metallurgy, mechanical alloying, additive manufacturing, and thin film deposition. The synthesis methods can affect the microstructure and properties of HEAs. One of the common methods to improve the chemical, physical, mechanical, and other properties of metals and alloys is rapid solidification. This method involves cooling the melt at rates above 10^4 K/s, which results in a wide range of metastable structural states in the alloys, including nanocrystalline and amorphous, with unique property combinations [7-9]. Hence, rapid solidification is a promising method to obtain HEAs with superior characteristics.

The AlCoCrCuFeNi alloy is a high-entropy alloy that has been extensively studied in the past two decades due to its outstanding thermal and mechanical properties [10-13].

Researchers frequently analyze the effect of varying component content on the properties of the alloy, obtained by various methods [10-13], including laser alloying [14,15]. However, in most of the studied alloys, the molar fraction of aluminum did not exceed 3. At the same time, previous research indicates that Al greatly increases the hardness of CoCrCuFeNi base HEA. Therefore, it is of interest to study an alloy in which the aluminum content exceeds this value, and, simultaneously, the entropy of mixing remains sufficiently high. The Al₄CoCrCuFeNi HEA was explored in the work [13], however, it was obtained by mechanical alloying of elemental powders. This study investigates how the cooling rate influences the structure, phase formation, and microhardness (H_{μ}) of melt-quenched Al₄CoCrCuFeNi HEA.

2. Experimental details

The high-entropy alloy Al_{44.45}Co_{11.11}Cr_{11.11}Cu_{11.11}Fe_{11.11}Ni_{11.11} (at.%) was synthesized from pure (99.9%) elements in the required proportion by casting under an argon atmosphere using a Tamman high-temperature electric furnace.

To achieve compositional homogeneity, the alloy was remelted five times and then cast into a copper mold to obtain a cylindrical ingot with a diameter of 10 mm. The cooling rate of the as-cast ingot was $\sim 10^2$ K/s. The ingot was then cut into slices, which were used to study the microstructure and phase composition of the alloy. After that the ingot was remelted and quenched into films using a splat-quenching technique, which involved the collision of molten droplets onto the inner surface of a hollow copper cylinder with a radius $R=135$ mm rotating at ~ 8000 rpm. The cooling rate of the films was calculated from the film thickness [6]. The following equation was used:

$$V = \frac{\alpha}{c\rho\delta}(T - T_0), \quad (1)$$

where V is the cooling rate, α is the heat transfer coefficient, ρ is the film density, c is the heat capacity of the film, T is the film temperature, T_0 is the ambient temperature, and δ is the film thickness. Considering that the melt-quenched (MQ) films had a thickness of ~ 40 μm , the cooling rate was estimated to be $\sim 10^6$ K/s. The crystal structures of the as-cast and melt-quenched (MQ) samples were characterized by X-ray diffraction (XRD) using a DRON-2.0 diffractometer with monochromatized Cu $K\alpha$ radiation. The XRD patterns were analyzed using the QualX2 software for qualitative phase identification [16]. The microhardness was measured using a PMT-3 microhardness tester at a load of 100 g. The microstructures of the as-cast and MQ samples were revealed by etching with a solution of hydrochloric (10ml) and nitric (30ml) acids for 3-10 sec and observed using a NEOPHOT-21 optical microscope.

3. Results and discussion

The phase formation in high-entropy alloys is usually characterized by two main criteria: the entropy of mixing (ΔS_{mix}) and the enthalpy of mixing (ΔH_{mix}). However, some additional parameters have been proposed to predict the phase composition of HEAs [1-4]. These parameters include the valence electron concentration (VEC), the thermodynamic parameter Ω , which considers the melting temperature, the entropy of mixing and the enthalpy of mixing, and the atomic size difference (δ) among the alloy components.

We calculated ΔS_{mix} , ΔH_{mix} , δ , VEC, and Ω for the Al₄CoCrCuFeNi HEA using the data from [17] (Tab. 1).

Table 1

Electronic, thermodynamic, and atomic-size parameters of the Al₄CoCrCuFeNi HEA

Alloy	ΔS_{mix} [J/(mol·K)]	ΔH_{mix} [kJ/mol]	Ω	VEC	δ [%]
Al ₄ CoCrCuFeNi	13.13	-11.46	1.59	6.22	6.15

Based on the value of valence electron concentration given in Tab.1, it can be expected that a solid solution with a BCC lattice will form in the alloy under study. At the same time, the value of the atomic size difference δ is quite large, which indicates the possibility of the formation of an ordered solid solution.

The XRD patterns (Fig. 1) revealed the phase composition and the crystal lattice parameters (Tab. 2) of the alloy under investigation.

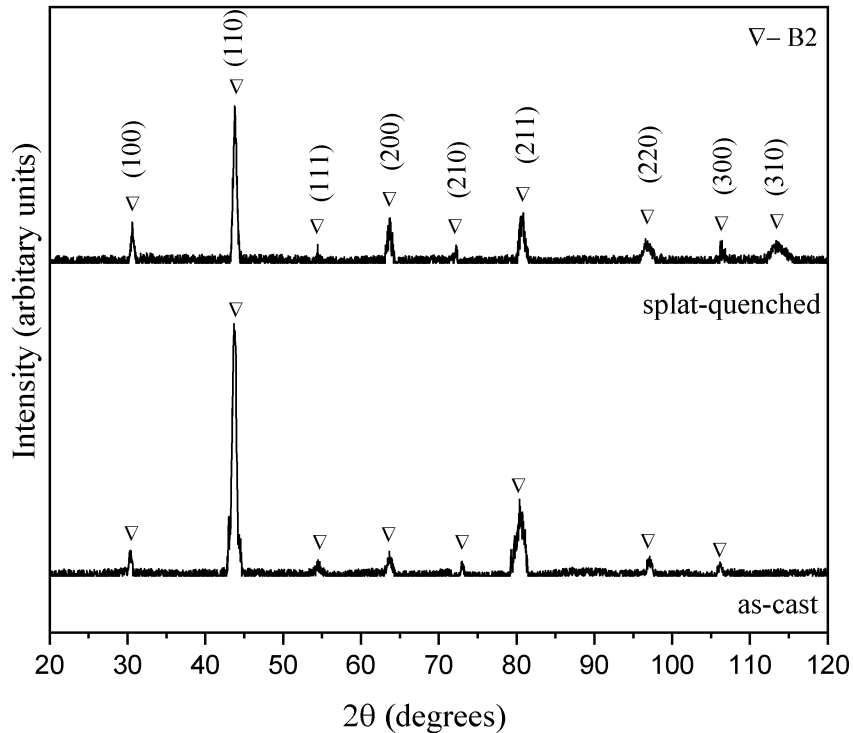


Fig. 1. XRD patterns of the Al₄CoCrCuFeNi high-entropy alloy.

Table 2

The phase composition of the Al ₄ CoCrCuFeNi HEA	
Alloy	Phase composition
As-cast Al ₄ CoCrCuFeNi	Ordered BCC (B2) +BCC ($a=0.2919$ nm)
MQ film Al ₄ CoCrCuFeNi	Ordered BCC (B2) ($a=0.2916$ nm)

X-ray diffraction patterns show that both as-cast and MQ samples contain the ordered BCC phase (B2). This confirms the applicability of the previously discussed theoretical criteria for predicting the phase composition of this alloy. At the same time, comparing XRD patterns, one can see that the intensity of superstructure peaks for MQ films is noticeably higher. The formation of the single BCC (B2) phase with an increase in the cooling rate of the melt and an increase in the Al concentration was also noted in AlCoCrCuFeNi alloy obtained by laser alloying [14,15].

If we consider the ratio of the integrated intensities $I^{(100)}/I^{(110)}$ of the XRD peaks corresponding respectively to a superstructure reflection (100) and fundamental reflection (110), then for a MQ film this ratio is 17.8 %, and for the as-cast sample only 5.4 %. Thus, it is obvious that the as-cast alloy, along with the ordered phase B2, must contain a certain proportion of the disordered BCC solid solution phase. At the same time, the MQ film obviously contains practically no disordered phase. This can be explained by the fact that at a

high cooling rate, the ordered phase formed in the MQ film at a sufficiently high temperature remains unchanged. In the as-cast sample, cooled at a low rate, there is enough time for diffusion processes to pass, and a high entropy of mixing will contribute to the decomposition of an ordered and the appearance of a disordered solid solution. This assumption is confirmed by the results of the work [18]. However, according to the model proposed in [19,20], the high ΔS_{mix} in this case is unable to stabilize a single-phase disordered solid solution because the enthalpies of formation of binary compounds AlNi (-677 meV/atom), AlCo (-629 meV/atom) and AlFe (-369 meV/atom) are too low [19]. All these compounds have an ordered B2 structure, and considering the value of formation enthalpy, it is obvious that the formation of the B2 phase in the $\text{Al}_4\text{CoCrCuFeNi}$ alloy occurs based on the AlNi compound ($a=0.2881$ nm). The presence of the B2 AlNi phase was previously confirmed in the alloys of the AlCoCrCuFeNi system [10,13,21]. The authors of work [22] proposed another mechanism for the transition of the ordered B2 phase into a combination of a disordered BCC phase and an ordered B2 phase - through spinodal decomposition. The likelihood of such decomposition in $\text{Al}_4\text{CoCrCuFeNi}$ alloy is confirmed by further studies of the microstructure of the as-cast sample. In a MQ film the decomposition process does not have time to proceed due to the high cooling rate.

Typical dendritic structures were observed in the as-cast sample of $\text{Al}_4\text{CoCrCuFeNi}$ high-entropy alloy (Fig. 2 a). Inside the dendrites, spinodal decomposition obviously takes place, as described in [10] for $\text{Al}_x\text{CoCrCuFeNi}$ HEAs with high aluminum content. At the same time, the microstructure of the melt-quenched film (Fig. 2 b) is a finely dispersed structure.

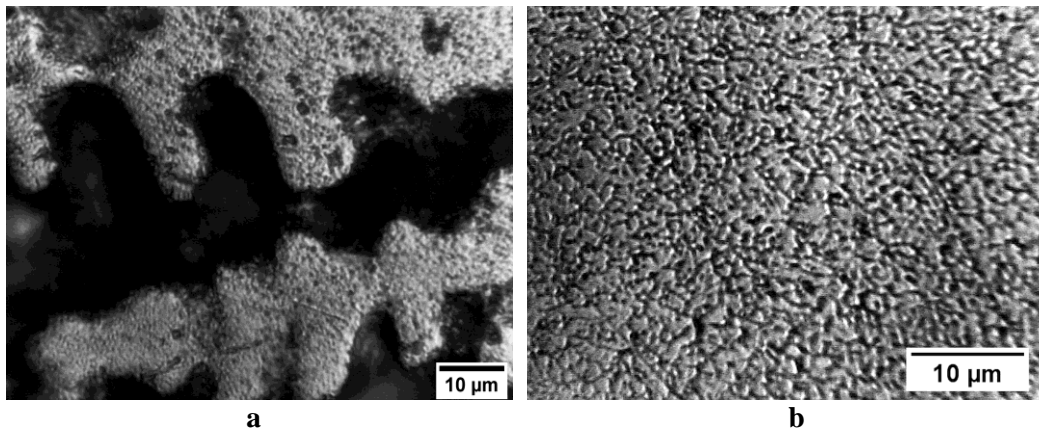


Fig. 2. Optical micrographs of the cross-section of as-cast (a) and melt-quenched (b) $\text{Al}_4\text{CoCrCuFeNi}$ HEA samples.

Observed structure transformation may be explained by the following: increasing of cooling rate (up to 10^6 K/s) leads to the degeneracy of dendritic structure and formation of the plane front of crystallization with finely dispersed structure occurrence.

High-resolution transmission and scanning electron microscopy studies reveal the fine structure of AlCoCrCuFeNi system HEAs, which consists of not only the phases detected by XRD but also various precipitates with different compositions and morphology [10]. These precipitates are either atomically ordered or disordered, and have nanoscale or sub-micron dimensions.

The substitutional solid solution of heterogeneous atoms with large differences in size, electronic structure, and thermodynamic properties induces high hardness in the alloys. The

crystal lattice undergoes considerable and statistically uniform distortion due to these differences, leading to significant hardening. In the alloy under study, the greatest distortions should be provided by aluminum atoms, as they are the most different in size from the rest of the alloy components. The microhardness of the as-cast HEA was measured to be H_{μ} =6500 MPa (averaged over dendritic and interdendritic regions), while the microhardness of the MQ HEA was significantly higher and reached H_{μ} =9400 MPa. Obviously, such an increase in the microhardness of MQ films is mainly due to an increase in the content of the hard and brittle ordered B2 phase in them. Similar values of microhardness were also obtained in Al₄CoCrCuFeNi alloy synthesized by mechanical alloying and spark plasma sintering [13]. Another reason for this difference in microhardness apparently consists in the fact that the MQ Al₄CoCrCuFeNi HEA films were far from the equilibrium state and had a microstructure that was characterized by a higher level of microdeformations, dislocation density, and smaller grain sizes, in contrast to the as-cast samples, which were in a more equilibrium state.

4. Conclusions

The influence of the cooling rate on the structure, phase formation, and microhardness of multicomponent high-entropy Al₄CoCrCuFeNi alloy was investigated. An analysis of the XRD patterns made it possible to establish that the structure of the as-cast alloy consists of an ordered B2 phase with a lattice parameter $a = 0.2919$ nm and a minor disordered BCC phase. When the melt quenching was performed, an ordered B2 phase remained in the alloy structure, and the lattice parameter changed to $a=0.2916$ nm. This confirms the applicability of the thermodynamic, electronic, and atomic-size criteria of phase formation discussed in the article for predicting the phase composition of Al₄CoCrCuFeNi alloy. The as-cast alloy sample displays a typical cast dendritic structure, while the microstructure of the melt-quenched film is a finely dispersed conglomerate of phases. The measured microhardness of the melt-quenched alloy reached 9400 MPa and significantly exceeded the microhardness of the as-cast alloy (6500 MPa). Thus, an increase in the cooling rate during quenching from the liquid state improves the mechanical properties of the Al₄CoCrCuFeNi high-entropy alloy.

References

1. **Srivatsan, T. S.** High entropy alloys. Innovations, advances, and applications / T. S. Srivatsan, M. Gupta. – Boca Raton : CRC Press, 2020. – 758 p.
2. **Brechtl, J.** High-entropy materials: theory, experiments, and applications / J. Brechtl, P. K. Liaw. – Cham : Springer International Publishing, 2021. – 774 p.
3. **Xiang H.** High- entropy materials. From basics to applications / H. Xiang, F.-Z. Dai, Y. Zhou. – Weinheim, Germany : Wiley – VCH GmbH, 2023. – 272 p.
4. **Miracle, D. B.** A critical review of high entropy alloys and related concepts / D. B. Miracle, O. N. Senkov // *Acta Materialia*. – 2017. – Vol. 122. – P. 448 – 511.
5. **Polonsky, V. A.** Structure and corrosion-electrochemical properties of Fe-based cast high-entropy alloys / V. A. Polonsky, V. F. Bashev, O. I. Kushnerov // *Journal of Chemistry and Technologies*. – 2020. – Vol. 28, No. 2. – P. 177 – 185.
6. **Polonsky, V.A.** Structure and corrosion-electrochemical properties of rapidly quenched Fe₅CrCuNiMnSi and Fe₅CoCuNiMnSi high entropy alloys / V.A. Polonsky, V.F. Bashev, O.I. Kushnerov // *J. Chem. Technol.* – 2022. – Vol. 30. – P. 88–95.
7. **Kushnerov, O. I.** Structure and properties of nanostructured metallic glass of the Fe–B–Co–Nb–Ni–Si high-entropy alloy system / O. I. Kushnerov, V. F. Bashev, S. I. Ryabtsev // *Springer Proceedings in Physics*. – 2021. – Vol. 246. – P. 557 – 567.

8. **Kushnerov, O. I.** Structure and physical properties of cast and splat-quenched CoCr_{0.8}Cu_{0.64}FeNi high entropy alloy / O. I. Kushnerov, V. F. Bashev // *East European Journal of Physics*. – 2021. – No. 3. – P. 43–48.
9. **Kushnerov, O.I.** Metastable states and physical properties of Co-Cr-Fe-Mn-Ni high-entropy alloy thin films / O.I. Kushnerov, S.I. Ryabtsev, V.F. Bashev // *Mol. Cryst. Liq. Cryst.* – 2023. – Vol. 750. – P. 135–143.
10. **Tong, C.-J.** Microstructure characterization of Al_xCoCrCuFeNi high-entropy alloy system with multiprincipal elements / C.-J. Tong, Y.-L. Chen, J.-W. Yeh [et al.] // *Metall. Mater. Trans. A*. – 2005. – Vol. 36. – P. 881–893.
11. **Plevachuk, Y.** AlCoCrCuFeNi-Based High-Entropy Alloys: Correlation Between Molar Density and Enthalpy of Mixing in the Liquid State / Y. Plevachuk, J. Brillo, A. Yakymovych // *Metall. Mater. Trans. A Phys. Metall. Mater. Sci.* – 2018. – Vol. 49. – P. 6544–6552.
12. **Liu, Y.Y.** The effect of Al content on microstructures and comprehensive properties in Al_xCoCrCuFeNi high entropy alloys / Y.Y. Liu, Z. Chen, J.C. Shi [et al.] // *Vacuum*. – 2019. – Vol. 161. – P. 143–149.
13. **Ziaei, H.** Phase evolution in mechanical alloying and spark plasma sintering of Al_xCoCrCuFeNi HEAs / H. Ziaei, B. Sadeghi, Z. Marfavi [et al.] // *Mater. Sci. Technol.* – 2020. – Vol. 36. – P. 604–614.
14. **Girzhon, V.V.** Analysis of structure formation processes features in high-entropy alloys of Al-Co-Cr-Fe-Ni system during laser alloying / V.V. Girzhon, V.V. Yemelianchenko, O.V. Smolyakov, A.S. Razzokov // *Results Mater.* – 2022. – Vol. 15. – P. 100311.
15. **Girzhon, V.** High entropy coating from AlCoCrCuFeNi alloy, obtained by laser alloying / V. Girzhon, V. Yemelianchenko, O. Smolyakov // *Acta Metall. Slovaca*. – 2023. – Vol. 29. – P. 44–49.
16. **Altomare, A.** Key features of Qualx2.0 software for qualitative phase analysis / A. Altomare, N. Corriero, C. Cuocci, A. Falcicchio, A. Moliterni, R. Rizzi // *Powder Diffraction*. – 2017. – Vol. 32, No. S1. – P. S129–S134.
17. **Takeuchi, A.** Classification of Bulk Metallic Glasses by Atomic Size Difference, Heat of Mixing and Period of Constituent Elements and Its Application to Characterization of the Main Alloying Element / A. Takeuchi, A. Inoue // *Mater. Trans.* – 2005. – Vol. 46. – P. 2817–2829.
18. **Priputen, P.** Unconventional order/disorder behaviour in Al–Co–Cu–Fe–Ni multi-principal element alloys after casting and annealing / P. Priputen, P. Noga, M. Novaković, J. Potočník, A. Antušek, R. Bujdák, E. Bachleda, M. Drienovský, M. Nosko // *Intermetallics*. – 2023. – Vol. 162. – P. 108016.
19. **Troparevsky, M.C.** Criteria for Predicting the Formation of Single-Phase High-Entropy Alloys / M.C. Troparevsky, J.R. Morris, P.R.C. Kent // *Phys. Rev. X*. – 2015. – Vol. 5. – P. 011041.
20. **Troparevsky, M.C.** Beyond Atomic Sizes and Hume-Rothery Rules: Understanding and Predicting High-Entropy Alloys / M.C. Troparevsky, J.R. Morris, M. Daene [et al.] // *JOM*. – 2015. – Vol. 67. – P. 2350–2363.
21. **Wang, Y.P.** Solid Solution or Intermetallics in a High-Entropy Alloy / Y.P. Wang, B.S. Li, H.Z. Fu // *Adv. Eng. Mater.* – 2009. – Vol. 11. – P. 641–644.
22. **Bai, K.** Unexpected spinodal decomposition in as-cast eutectic high entropy alloy Al₃₀Co₁₀Cr₃₀Fe₁₅Ni₁₅ / K. Bai, C. K. Ng, M. Lin, B. Cheng, Y. Zeng, D. Wu, J. J. Lee, S. L. Teo, S. R. Ng, D. C. C. Tan, P. Wang, Z. Aitken, Y.-W. Zhang // *Materials & Design*. – 2023. – Vol. 236. – P. 112508.